Increases in flood magnitudes in California under warming climates

Tapash Das [a,b,*], Edwin P. Maurer [c], David W. Pierce [b], Michael D. Dettinger [d,b], Daniel R. Cayan [b,d]

[a] CH2M HILL, Inc., San Diego, CA, USA
[b] Division of Climate, Atmospheric Sciences, and Physical Oceanography, Scripps Institution of Oceanography, La Jolla, CA, USA
[c] Santa Clara University, CA, USA
[d] United States Geological Survey, La Jolla, CA, USA

ARTICLE INFO

SUMMARY

Downscaled and hydrologically modeled projections from an ensemble of 16 Global Climate Models suggest that flooding may become more intense on the western slopes of the Sierra Nevada mountains, the primary source for California's managed water system. By the end of the 21st century, all 16 climate projections for the high greenhouse-gas emission SRES A2 scenario yield larger floods with return periods ranging 2–50 years for both the Northern Sierra Nevada and Southern Sierra Nevada, regardless of the direction of change in mean precipitation. By end of century, discharges from the Northern Sierra Nevada with 50-year return periods increase by 30–90% depending on climate model, compared to historical values. Corresponding flood flows from the Southern Sierra increase by 50–100%. The increases in simulated 50 year flood flows are larger (at 95% confidence level) than would be expected due to natural variability by as early as 2035 for the SRES A2 scenario.

© 2013 Elsevier B.V. All rights reserved.

1. Introduction

Hydrometeorological extremes often have major impacts on human activities, water resources, agricultural activities, urban infrastructure and ecosystems. Floods in particular damage human infrastructure, take many lives globally and are one of the costliest types of natural disaster in economic and human terms (Bouwer and Vellinga, 2003). California, our focus here, has suffered many severe floods historically (Kelley, 1998) with annual damages averaging over $350 million (Pielke et al., 2002). California is highly vulnerable to floods because its dense communities and infrastructure in low lying areas (Lund, 2012).

California is characterized by a Mediterranean seasonal climate with precipitation falling almost entirely in the Winter (December–February) and Spring (March–May) (Cayan et al., 1998). Floods in California are typically associated with specific winter-spring atmospheric circulations (Cayan and Riddle, 1992), and recent research suggests relationships of atmospheric rivers with the largest floods in California (Ralph et al., 2006; Neiman et al., 2007; Dettinger and Ingram, 2013). In response to continuing increases in global greenhouse-gas emissions, California at the end of the

twenty-first century is projected to experience warming by 1.5–4.5 °C (Cayan et al., 2008a,b). There are uncertainties about future changes in long-term average precipitation rates in California (e.g., Dettinger, 2005; Cayan et al., 2008a,b). At the seasonal level, the ensemble mean projected changes in precipitation for the mid-late 21st century have been shown to favor wetter winters and drier springs (Pierce et al., 2013a). These winter precipitation increases are largely driven by increases in daily precipitation intensity more so than the number of days with precipitation (Pierce et al., 2013b). It is projected that even though the overall frequency of precipitation events may decrease in many areas of California, there may be increases in the largest precipitation events (Easterling et al., 2000; Pierce et al., 2013a, 2013b).

With more water vapor and heat in the atmosphere, it is anticipated that storms will yield greater peak precipitation rates, and thus floods may become more intense in many areas (e.g., Trenberth, 1999; Milly et al., 2002; Kunkel et al., 2013). Indeed, there is already observational evidence that precipitation extremes have increased in many parts of the world (Groisman et al., 2005) and in some cases these increases have been attributed to human driven greenhouse gas increases (Min et al., 2011). However, as the polar regions are expected to warm more quickly than the lower latitudes, the equator-to-pole temperature differences would decline (Jain et al., 1999) which generally is expected to weaken

* Corresponding author at: CH2M HILL, Inc., San Diego, CA, USA. Tel.: +1 (619) 272 7272; fax: +1 (619) 687 0111.
E-mail address: tapash.das@ch2m.com (T. Das).

mid latitude storm tracks of the sort that brings California dangerous storms.

The combination of these two conflicting tendencies (more moisture in the atmosphere yielding larger peak precipitation rates and weakened storm tracks reducing the power and opportunities for large storms) has left the future of flooding in California uncertain. Several studies have projected possibilities of more floods in California under climate change (e.g., Miller et al., 2003; Dettinger et al., 2004, 2009; Anderson et al., 2006; Raff et al., 2009; Das et al., 2011) but a more exhaustive evaluation of possible climatic futures has been lacking.

We describe here, for two primary catchments in California, potential changes in annual maximum 3-day flood discharges under a wide range of projected climate changes provided by a large ensemble of climate projections.

The 3-day peak flow is a widely used measure for flood planning purposes in California, and one that has been used in prior climate change impacts studies (CA DWR, 2006; Chung et al., 2009; Das et al., 2011). Das et al. (2011) found a robust increase in 21st century 3-day peak flow magnitudes based on output from three Global Climate Models (GCMs) using a single greenhouse gas emission scenario and output from three GCMs. In this study we expand this analysis to include two emissions scenarios, one with high (SRES A2, as in Das et al., 2011) and one with lower atmospheric concentrations of greenhouse gases (SRES B1) through the 21st century, and an ensemble of 16 GCMs (Table 1) from the World Climate Research Program's (WCRP) Coupled Model Intercomparison Project phase 3 (CMIP3), a number adequate to account for the effects of the natural internal climate variability and most model-to-model scatter among the GCMs. The study also performs a broader evaluation of how flood changes track changes in annual streamflows and precipitation. This evaluation is critical given continuing uncertainties in projected annual precipitation in the study area. Using this ensemble we are able to identify robust projections in flood magnitudes for different return periods. This analysis will help quantify the changes in these floods in ways that are informative to policymakers as they contemplate design recommendations for increases in the magnitudes of design floods (e.g., CA DWR, 2008) or changes in the design recurrence interval (Mailhot and Duchesne, 2010) as adaptation responses to increased flood risk.

2. Data, models and methods

2.1. Study area and data

The study area consists of the western slopes of the Northern and Southern Sierra Nevada mountains (Fig. 1). The Sierra Nevada are the primary sources of inflows to California's Central Valley, with about 40% of the State's total flows deriving from the range (Morandi, 1998). Flows from the Sierra Nevada provide about one-third of the water supplies serving about 25 million people across the entire length of the State and irrigation supplies for at least $36 billion/year in agriculture (Service, 2007; USDA, 2011). However, in addition to being the largest water supply source for the State, rivers from the Sierra Nevada have also, throughout history and prehistory, been the sources for devastating floods in the Central Valley (Dettinger and Ingram, 2013). The management of flows from the range have always been challenged by the tension between their value as water supplies and the risks they pose as major flood generators, a tension that may be greatly aggravated if flood risks increase with the changing climate.

The Northern Sierra catchment includes the drainage areas of the Sacramento River at Bend Bridge, the Feather River at Oroville and the Yuba River at Smartville. Streamflows from the Northern Sierra feed into Sacramento River. The Southern Sierra catchment is defined here to consist of the tributary drainages of the San Joaquin River: the Stanislaus at New Melones Dam, the Tuolumne River at New Don Pedro, the Merced at Lake McClure, and the San Joaquin at Millerton Lake.

We used observed, gridded fields of daily maximum and minimum temperature (T_{min}, T_{max}) and precipitation (P) from the Surface Water Modeling Group at the University of Washington (http://www.hydro.washington.edu). The data have a spatial resolution of 1/8° (approximately 12 km per grid cell) and are derived from two different sources: Maurer et al. (2002) and Hamlet and Lettenmaier (2005). Both the Maurer et al. (2002) and Hamlet and Lettenmaier (2005) datasets used US National Oceanic and Atmospheric Administration (NOAA) Cooperative Observer (Co-op) stations. However, the Hamlet and Lettenmaier (2005) dataset focused more on the Historical Climatology Network (HCN) (Easterling et al., 1996) subset of Co-op stations. HCN

Table 1
GCM modeling group, GCM name and GCM abbreviation used in this study.

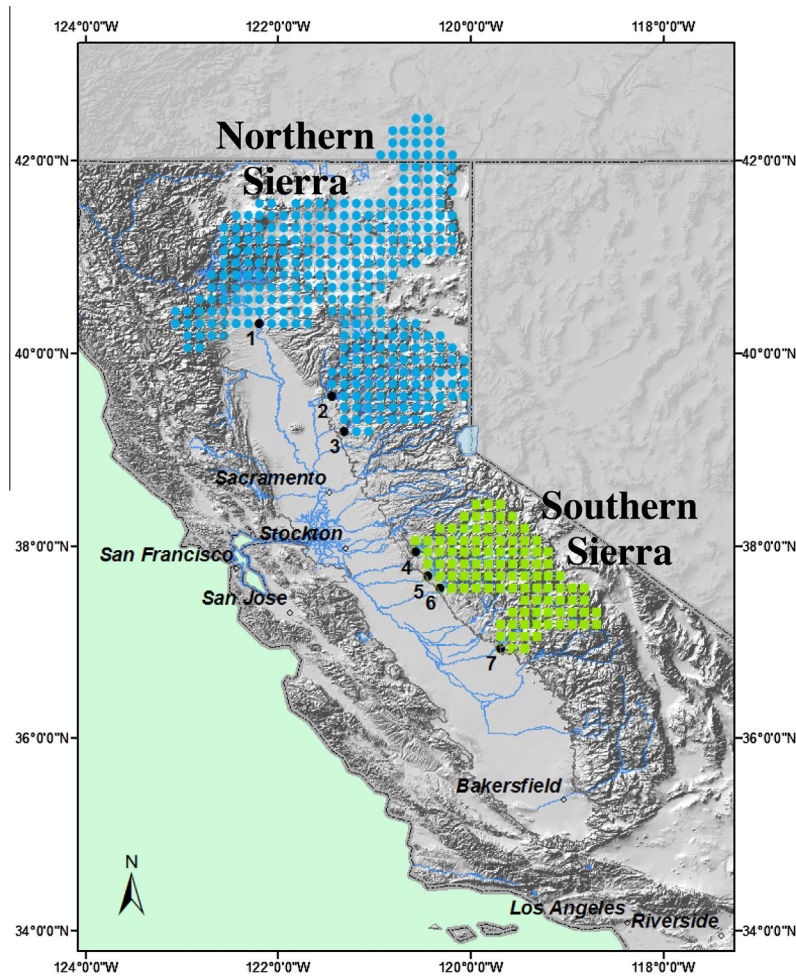| GCM Modeling Group, Country	WCRP CMIP3 I.D.	GCM abbreviation used in this study
Bjerknes Centre for Climate Research, Norway	BCCR-BCM2.0	bccr-bcm2.0.1
Canadian Centre for Climate Modeling & Analysis, Canada	CGCM3.1 (T47)	cccma-cgcm3.1.1
Meteo-France/Centre National de Recherches Meteorologiques, France	CNRM-CM3	cnrm-cm3.1
CSIRO Atmospheric Research, Australia	CSIRO-Mk3.0	csiro-mk3.0.1
US Dept. of Commerce/NOAA/Geophysical Fluid Dynamics Laboratory, United States	GFDL-CM2.0	gfdl-cm2.0.1
US Dept. of Commerce/NOAA/Geophysical Fluid Dynamics Laboratory, United States	GFDL-CM2.1	gfdl-cm2.1.1
NASA/Goddard Institute for Space Studies, United States	GISS-ER	giss-model-e.r.1
Institute for Numerical Mathematics, Russia	INM-CM3.0	inmcm3.0.1
Institut Pierre Simon Laplace, France	IPSL-CM4	ipsl-cm4.1
Center for Climate System Research (The University of Tokyo), National Institute for Environmental Studies, and Frontier Research Center for Global Change (JAMSTEC), Japan	MIROC3.2 (medres)	miroc3.2-medres.1
Meteorological Institute of the University of Bonn, Germany and Institute of Korea Meteorological Administration, Korea	ECHO-G	miub-echo-g.1
Max Planck Institute for Meteorology, Germany	ECHAM5/ MPI-OM	mpi-echam5.1
Meteorological Research Institute, Japan	MRI-CGCM2.3.2	mri-cgcm2.3.2a.1
National Center for Atmospheric Research, United States	CCSM3	ncar-ccsm3.0.1
National Center for Atmospheric Research, United States	PCM	ncar-pcm1.1
Hadley Centre for Climate Prediction and Research/Met Office, United Kingdom	UKMO-HadCM3	ukmo-hadcm3.1

Fig. 1. California's Northern Sierra Nevada and Southern Sierra Nevada. The northern Sierra Nevada consists of the drainage areas from the Sacramento River at Bend Bridge (1), the Feather River at Oroville (2) and the Yuba River at Smartville (3). The Southern Sierra Nevada consists of the drainage areas from the four main tributaries of the San Joaquin river: the Stanislaus at New Melones Dam (4), the Tuolumne River at New Don Pedro (5), the Merced at Lake McClure (6) and the San Joaquin at Millerton Lake (7).

stations are chosen and corrected to eliminate most temporal inhomogeneities in Hamlet and Lettenmaier (2005), whereas the Maurer et al. (2002) dataset treated all stations more or less equally. Both datasets use monthly Precipitation-elevation Regressions on Independent Slopes Model (PRISM) data fields (Daly et al., 1994) to adjust for elevation effects on precipitation. Wind speed was interpolated to 1/8° from the National Centers for Environmental Prediction/National Center for Atmospheric Research (NCEP–NCAR) reanalysis (Kalnay et al., 1996) in both datasets.

The prospect of continued and intensifying climate change has motivated the assessment of impacts at the local to regional scale, which requires the use of downscaling methods to translate large-scale General Circulation Model (GCM) output to regionally more-relevant scales (Carter et al., 2007; Christensen et al., 2007). Downscaling is typically categorized into two types: dynamical, using a higher resolution climate model that better represents the finer-scale processes and terrain in the region of interest; and statistical, where relationships are exploited between large scale climate statistics and those at finer scales (Fowler et al., 2007). While dynamical downscaling has the advantage of producing complete, physically consistent fields, its computational demands preclude its common use when analyzing projections from multiple GCMs in a climate change impact assessment; we thus focus our attention on statistical downscaling.

The Bias Correction and Spatial Disaggregation (BCSD) technique used in this study was originally developed by Wood et al.

(2002) for using global model forecast output for long-range streamflow forecasting. The technique was later adapted for long-term climate projections (Wood et al., 2004). It has subsequently been widely used to downscale GCM output over regional areas (e.g. Hayhoe et al., 2007; Pierce et al., 2013a), continents (Maurer et al., 2007), and globally (e.g., Girvetz et al., 2009). The method begins with a quantile mapping approach (Panofsky and Brier, 1968) to correct for large scale biases in monthly precipitation and temperature, an approach that has been shown to be effective in reducing biases in climate model output (Themeßl et al., 2012) and specifically for studies of climate impacts on hydrology (Boé et al., 2007). For each of the 12 months, cumulative distribution functions (CDFs) are constructed for each GCM-scale grid cell for both the gridded observations and each GCM for the climatological period, 1950–1999 for this study. Using a monthly time series, each month is taken in turn for the entire GCM simulation (through the 21st century), and the quantile determined (independently for precipitation and temperature) using the CDF for the GCM for the current month. Each variable is then mapped to the same quantile for the observationally based CDF. For temperature the linear trend is removed prior to this bias correction and replaced afterward, to avoid increasing sampling at the tails of the CDF as temperatures rise. Since the projected changes in precipitation are generally within the bounds of historical observational variability, trend removal and replacement is not applied to precipitation. The spatial disaggregation is as described by

Wood et al. (2002), where the bias corrected GCM anomalies, expressed as a ratio (for precipitation) and shift (for temperature) relative to the 1950–1999 period at each large-scale GCM grid cell are interpolated to the centers of 1/8° hydrologic model grid cells over California. These factors are then applied to the 1950–1999 average gridded precipitation and temperature at the 1/8° scale. To recover daily values, for each month in the simulation a month is randomly selected from the historic record (the same month is used, so for a simulated January, a January is selected from the 1950–1999 period). Each day in that month's precipitation is scaled and temperature is shifted so that the monthly average matches the bias-corrected, interpolated GCM monthly value. The same historic month is used throughout the domain to preserve plausible spatial structure to daily storms.

Historical temperature and precipitation and downscaled changes in the two catchments studied here had been examined previously by Das et al. (2011). Two greenhouse gas emissions scenarios were studied here, the lower-emission B1 and higher-emission A2 pathways. The large ensemble of outputs from 16 GCMs under the two pathways each allows us to assess two types of uncertainty, the uncertainties due to unknown future greenhouse gas concentrations and due to imperfect modeling of how climate will respond (Hawkins and Sutton, 2009). This same set of GCM runs has been used in other recent climate change studies in the region (Ficklin et al., 2012; Pierce et al., 2013a).

2.2. Hydrologic model

The Variable Infiltration Capacity (VIC) hydrological model (Liang et al., 1994; Cherkauer et al., 2003) was used to simulate daily runoff and baseflow during the historical period and under 21st Century climate change conditions. The VIC model is a physically based, semi-distributed grid-based model that simulates the processes, driven by spatially explicit descriptions of land surface topography, soils, and vegetation, controlling the generation of runoff. It includes an energy balance snow accumulation and ablation model, which explicitly represents the interactions of snow and vegetation. The model simulates three soil layers and 5 elevation bands to account for the effects of sub-grid variability in topography. The VIC model was run at a daily time step in water balance mode at 1/8° spatial resolution (approximately 12 km per grid cell). The snow-model within the VIC was run at 1 h time step. In this implementation, the VIC model was run over the study area using the same parameterization as in prior work including Maurer (2007), Barnett et al. (2008), Hidalgo et al. (2009), Maurer et al. (2010), and Das et al. (2011). Prior work has assessed the VIC model performance (with the same parameterization as in this study), comparing observed flows with those simulated by VIC being driven by the gridded observed meteorology as used in this study. For example, biases were below 10% for VIC simulation streamflow for tributary rivers included in the study areas used here (Maurer, 2007) and the correlation coefficient between VIC and observed streamflow was well above 0.9 (Hidalgo et al., 2009). For the larger aggregated Northern Sierra Nevada and Southern Sierra Nevada used in this study, we found for the 1950–1999 period observed streamflows were well simulated, with biases below 5%. .

2.3. Methods

VIC simulated runoff and baseflow are combined and routed to basin outlets obtain daily streamflows for the study by the method of Lohmann et al. (1996). While some studies investigating climate change impacts on flooding look at changing frequencies of floods of specified magnitude (e.g., Milly et al., 2002), we focus instead on changes in the magnitude of floods with specified recurrence inter-

vals. As in Das et al. (2011), first, for every member of the ensemble of routed flows, 3-day maximum discharges were identified for every year. The probabilities of exceedance (assigned using the Weibull plotting position) for various return periods were estimated for 1951–1999, 2001–2049, and 2051–2099 using the 3-day maximum discharges. Since empirical Weibull plotting positions based on 50-year periods are inadequate by themselves to estimate the probability of exceedence of relatively rare events, we fit them to a standard theoretical frequency distribution to compare the flood magnitudes for specific frequency events between the historic period, and the 2001–2049, and 2051–2099 periods. To do this, an inverse of the probability (frequency factor, K; Chow et al., 1988) was calculated for each ensemble member and study period. A log-Pearson type III distribution (USGS, 1981; Reis et al., 2005; Griffis and Stedinger, 2007) was assumed as the theoretical distribution in the calculation. K values were plotted against the base 10 logarithm of the 3-day streamflow maxima. Flood discharges with different return periods ranging from 2 years through 50 years were estimated for each of the periods for each ensemble member from these log-Pearson type III frequency estimates.

3. Results

The flood frequency curves obtained using VIC driven by downscaled historical climate models fall reasonably well within the spread of those obtained when VIC is driven by the Maurer et al. (2002) and Hamlet and Lettenmaier (2005) observational data sets (Fig. 2). In the remainder of the paper we proceed using only the Hamlet and Lettenmaier (2005) data set, since our flood results using the two observed data sources are not different at the 5% significance level based on the two-sample Kolmogorov–Smirnov test (Haan, 2002).

The 16 GCM simulations of historic and projected (SRES A2) annual 3-day peak flows are shown in Fig. 3, wherein the high variability of year-to-year values of 3-day peak flows is evident. Nonetheless, the median of the ensemble has more high values later in the 21st century than in the historic period for Northern Sierra. The 75th percentile of the ensemble increases considerably later in the 21st century than in the historic period for both the Northern and Southern Sierra Nevada, with larger increases in the latter. The 25th percentile, by contrast, does not display an obvious trend in either basin. What this indicates is that variability in peak flow projections among ensemble members increases through the 21st century, but this increased variability is manifested in one direction – toward more model projections for extreme high peak flows. To quantify these changes in the context of a peak flow events used in engineering design, Fig. 4 shows the 50-year peak 3-day floods for the Northern and Southern Sierra for the SRES A2 emissions scenario in two 49-year windows. A 50-year flood is of practical interest because it surpasses many thresholds in natural and managed systems, and because the rising potential for flood damages due to exceeding capacities of roadway and urban storm drainage systems.

Most notable in Fig. 4 is that, among the early 21st century GCM projections (bottom panels), only three of 16 ensemble members yield declines in the 50-year flood events from the Northern Sierra, and only two in the southern Sierra. This consensus of increasing flood magnitudes occurs even though approximately half of the projections yielded reduced mean precipitation rates (relative to the late 20th century historic period), as indicated by the colors of the dots in Fig. 4. By the second half of the 21st century (top panels, Fig. 4), all 16 projections yield increased 50-year flood magnitudes.

Fig. 5 summarizes the results for other return periods, and shows that this finding is not limited to the 50-year event. With
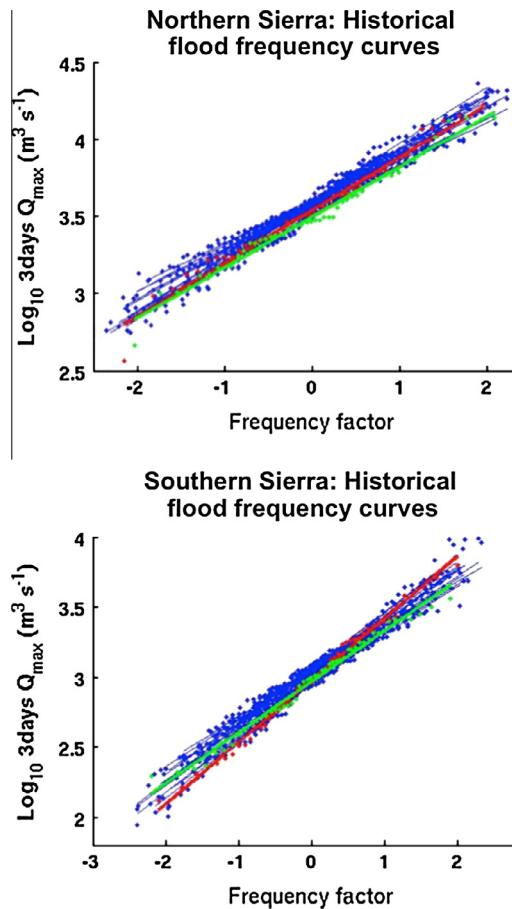
Northern Sierra: Historical flood frequency curves

Southern Sierra: Historical flood frequency curves

Fig. 2. Flood frequency curves constructed using 3-days annual maximum streamflows for Northern Sierra and Southern Sierra from VIC simulations as simulated by downscaled climate model meteorologies and observational meteorologies. In the plots, blue color curves are from model simulated historical period (1951–1999). Green color curve is from Hamlet and Lettenmaier (2005) observational driven simulation. Red color curve is from Maurer et al. (2002) observational driven simulation. (For interpretation of the references to color in this figure legend, the reader is referred to the web version of this article.)

the exception of the 2-year return period, at least 75% of all ensemble members yielded increased flood magnitudes for all recurrence intervals tested. Again this is despite the fact that the projections are more or less evenly divided between increases and decreases in mean annual precipitation and streamflow.
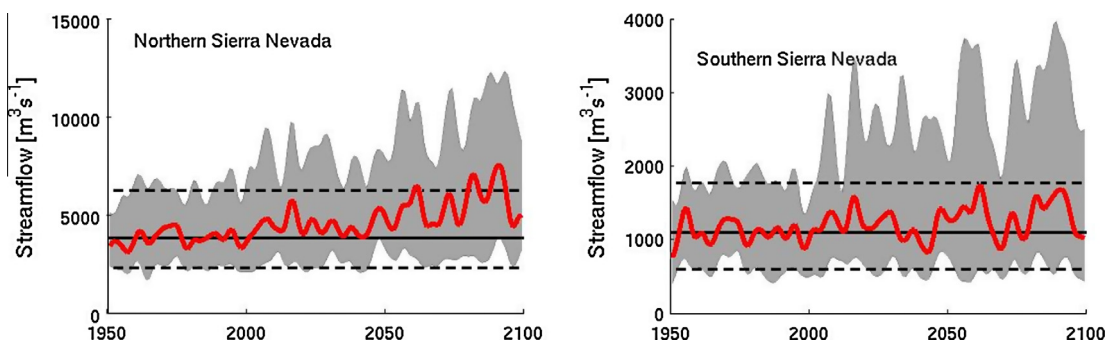
Fig. 6 shows the evolution of the ensemble of 50-year flood estimates through the 21st century. The ensemble median flood magnitude increases progressively through the 21st century, more so in the southern Sierra and under the SRES A2 emission scenario than in the northern Sierra or under B1 emissions. For the 49-year window centered near 2030 under SRES A2 emissions, the ensemble-median 50-year, 3-day flood flows have increased by more than the 95% confidence interval of natural variability in both Northern and Southern Sierra Nevada. The natural variability was characterized from VIC responses to a 750-year control climate simulation by National Center for Atmospheric Research Parallel Climate Model (PCM) described by Barnett et al. (2008). This suggests that, in the median, change in flood magnitudes may arise that would be confidently attributable to the human-induced greenhouse gas levels of the SRES A2 scenario within a few decades. For the SRES B1 emissions pathway, this degree of increase in peak flows is not attained until late in the 21st century for the Southern Sierra, and is not achieved during the 21st century for the Northern Sierra. This illustrates the potential benefits in terms of reduced flooding from reducing emissions but also shows the uncertainties that arise because we do not yet know what will be the future pathway that emissions follow.

Under the SRES A2 scenario, for the Northern Sierra, the 25th percentile ensemble range exceeds the 5% significance line for flood changes by early in the 21st century, indicating that more than 75% of the ensemble members yield 50-year flood increases by the 49-year window centered on 2025. For the Southern Sierra, this threshold is exceeded by 2005–2010. Although this might appear to suggest that we have likely already passed the time when 50-year flood peaks should have increased in magnitude (as we are presently much closer to the SRES A2 pathway; Friedlingstein et al., 2010), for such relatively rare events as the 50-year flood, with only a 2% chance of occurring in any year, detecting this change in the observational record may not be possible for years or decades. Also, of course, we are not at the end of the 49-year window centered on 2005–2010.

To examine the major driver for these changes in flood magnitude, Fig. 7 shows changes in precipitation over various intensity thresholds. The dominant change in precipitation is an increase in intense rain events, rather than in the number of days with rainfall. Whether precipitation falls as rain or snow also has a strong bearing on the potential for flooding, and observations indicate that changes toward a greater proportion of precipitation falling as rain instead of snow are occurring in this region (Knowles et al., 2006). The number of winter days with precipitation occurring as snow divided by the total number of winter days with precipitation, in the period November through March, was calculated
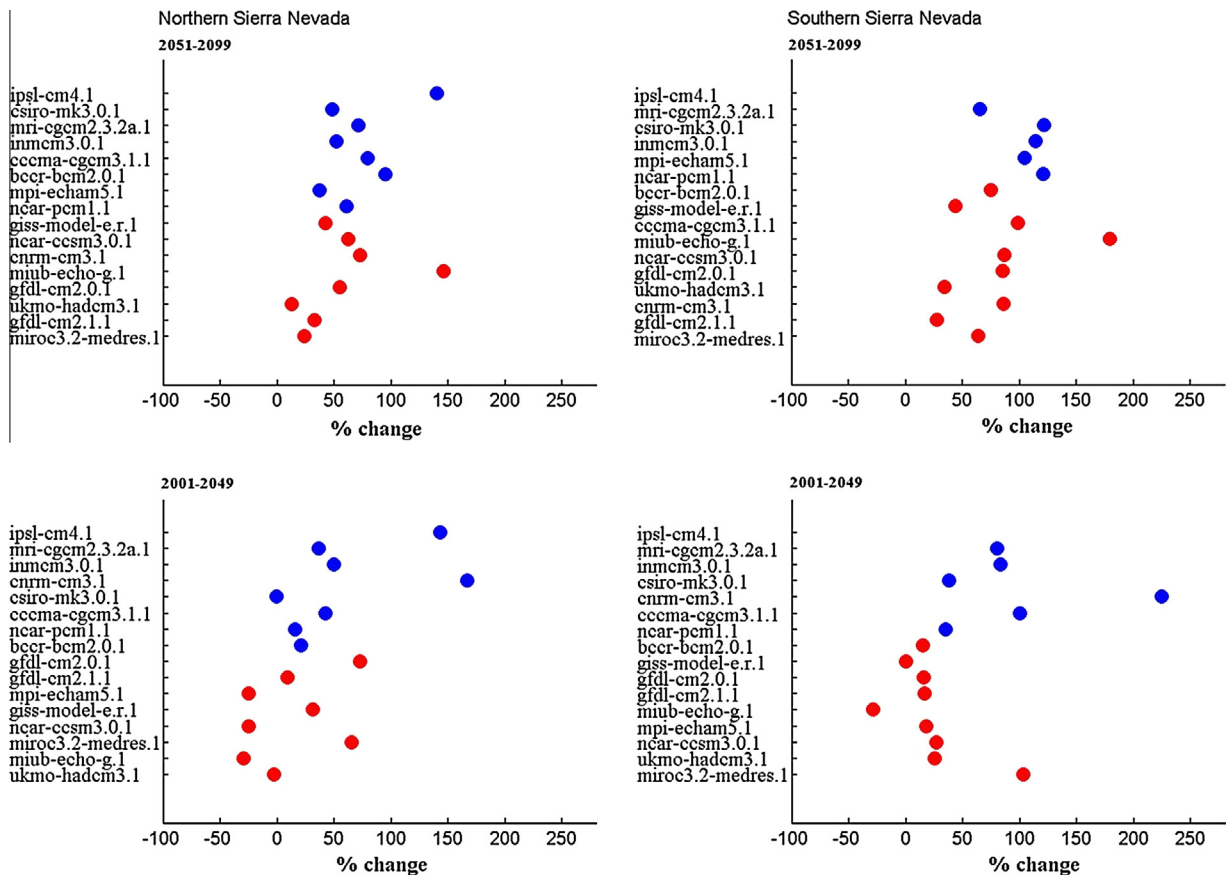

Fig. 3. VIC simulated 3-days annual maximum streamflows as driven by downscaled meteorologies from 16 global climate models. The median (red line) and 25th and 75th percentiles (gray shading) are shown from the simulated streamflows distribution among the 16 models. Black color horizontal lines represent median (solid black line), 25th and 75th percentiles (dotted black lines) computed over the climate model simulated historical time period 1951–1999. Results are smoothed using low pass filter shown from high emission scenario (SRES A2). Left) for Northern Sierra Nevada, Right) for Southern Sierra Nevada. (For interpretation of the references to color in this figure legend, the reader is referred to the web version of this article.)

Fig. 4. Percentage change in 50-year (2% exceedence) flood flows computed from VIC simulations driven by downscaled meteorologies from 16 global climate models. Changes are computed with respect to model simulated historical period 1951–1999 for each of the simulations. The solid vertical lines show the ensemble-median changes. 25th and 75th percentiles values are represented by dotted vertical lines. Climate models on *y*-axis are sorted by projected changes in mean annual precipitation, with driest at bottom and wettest at top. Dry models (that project decreasing annual precipitation) are indicated with reddish dots and wet models with blue. Results are shown from the high emission scenario (SRES A2). Result for ipsl-cm4.1 for Southern Sierra Nevada is not shown because the result is out of the range considered in the plot. Left panels: for Northern Sierra Nevada. Right panels: for Southern Sierra Nevada. (For interpretation of the references to colour in this figure legend, the reader is referred to the web version of this article.)
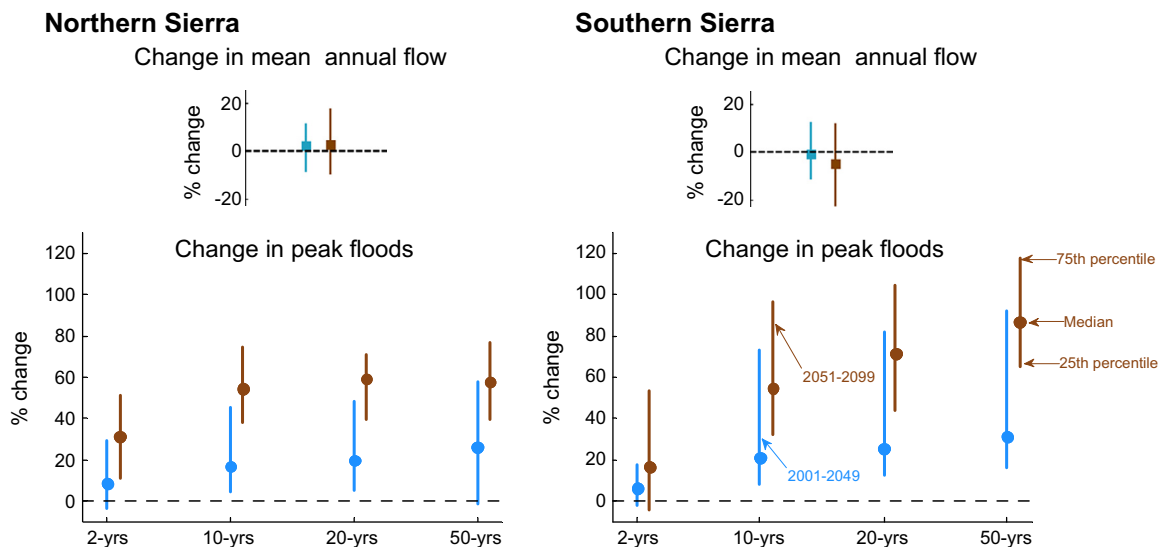

Fig. 5. Top panels: Range of percentage changes (relative to 1951–1999) in mean annual streamflow from VIC simulations as simulated by downscaled climate models. Bottom panels: Percentage changes of flood magnitudes for selected return periods. For each of the return periods, filled squares represent ensemble medians, and vertical whiskers extend from 25th to the 75th percentile of the 16 climate model samples. Changes in the period 2001–2049 (cyan) and 2051–2099 (dark red) are shown side by side. Results are shown from high emission scenario (SRES A2). Left panels are for Northern Sierra Nevada and right panels for Southern Sierra Nevada. (For interpretation of the references to color in this figure legend, the reader is referred to the web version of this article.)
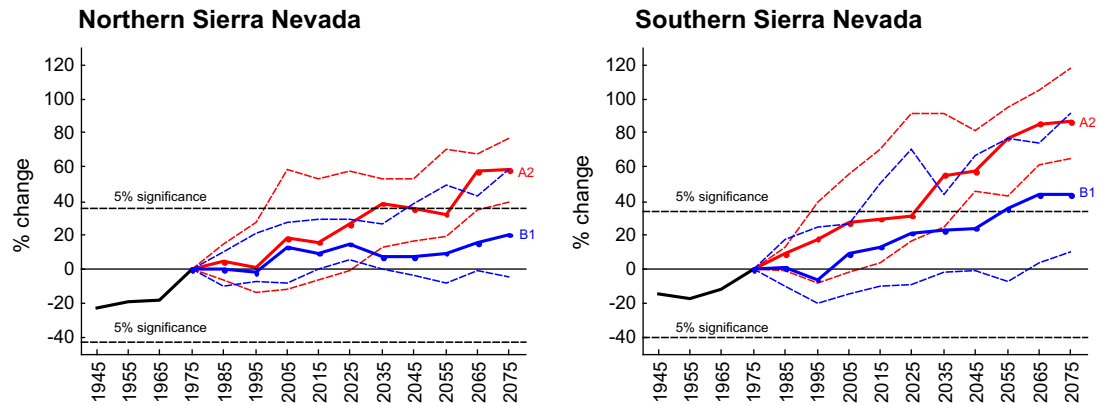
Fig. 6. Percentage changes of 50-years (2% exceedence) flood discharge (relative to floods from the 1951–1999 period) in moving, overlapping 49-year windows. The second, third and next on points are computed for the period with 10-years sliding period (e.g., the second point represents change of the flood magnitude computed for the 1931–1979 period with respect to flood discharge computed in the period 1951–1999). The plot shows 25th, 50th and 75th percentiles from 16 climate models from SRES A2 (red color curves) and SRES B1 (blue color curves) simulations for Northern Sierra Nevada (left) and Southern Sierra Nevada (right). In the plot, black color curves show the% change in 50-years flood with respect to historical flood (1951–1999) from VIC simulation as simulated by historical observed meteorologies (Hamlet and Lettenmaier, 2005). The 5% significant levels were computed using a long control simulation (750-years) from NCAR PCM1 and are shown as dotted gray horizontal lines. Numbers on the *x*-axis are the middle year of each 49-years time window used to estimate flood magnitudes. Note the changes over the periods 1921–1969, 1931–1979 and 1941–1989 are computed only from historical observed meteorologies driven VIC simulation. (For interpretation of the references to color in this figure legend, the reader is referred to the web version of this article.)
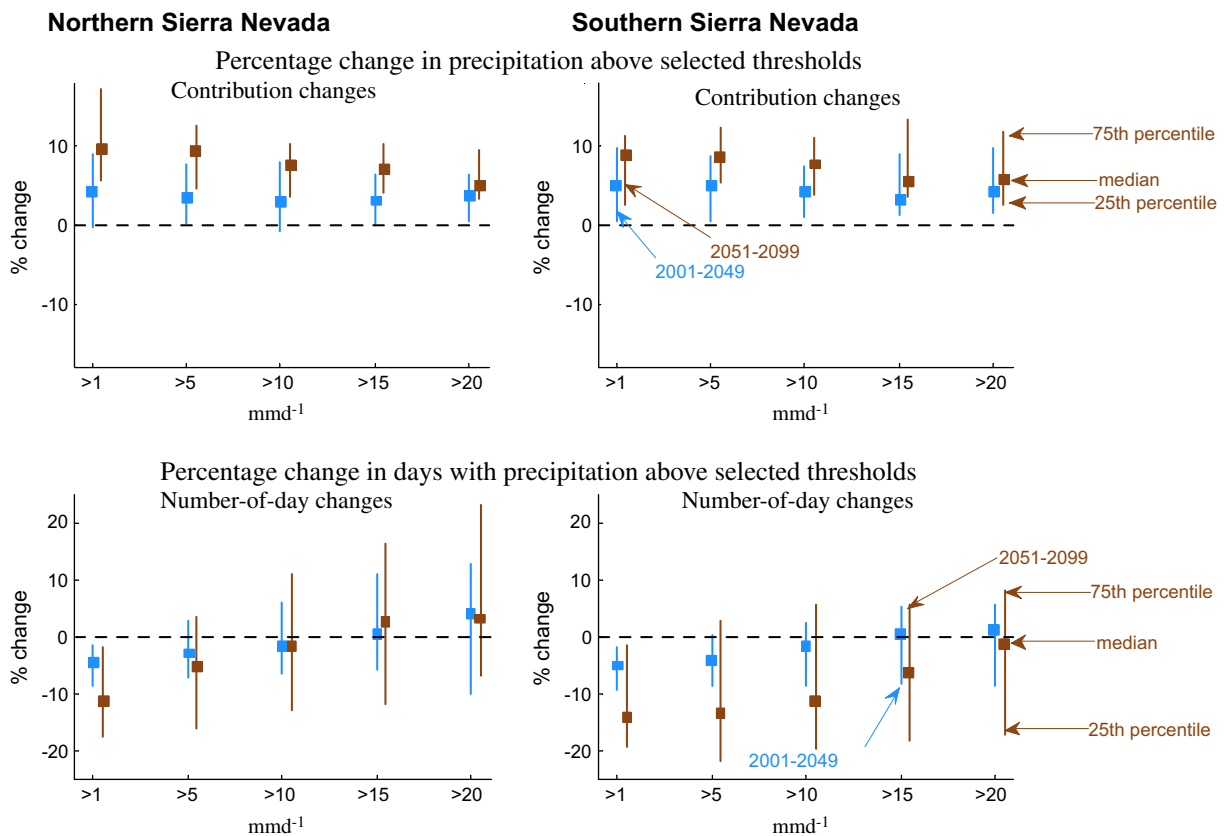

Fig. 7. Top panels: Percentage changes in (downscaled) precipitation amount above selected thresholds, from 16 global climate models. Bottom panels: Percentage changes in numbers of days with having precipitation above selected daily thresholds. Changes are relative to model-simulated historical 1951–1999 periods. For each of the selected thresholds, filled squares represent ensemble medians, and vertical whiskers extend from 25th to the 75th percentile of the 16 projections. Changes in the period 2001–2049 and 2051–2099 are shown side by side. Results are shown from high emission scenario (SRES A2). Left panels are for Northern Sierra Nevada, and right panels are for Southern Sierra Nevada.

following a procedure implemented in VIC (Cherkauer et al., 2003) using days when portion of the precipitation falls as liquid rainfall or portion of the precipitation turns into snow as compared to total

wet days (days with precipitation larger than 0.1 mm). This definition, based on air temperatures, is a proxy for the fractions of precipitation that are frozen and unfrozen (snow and rain)
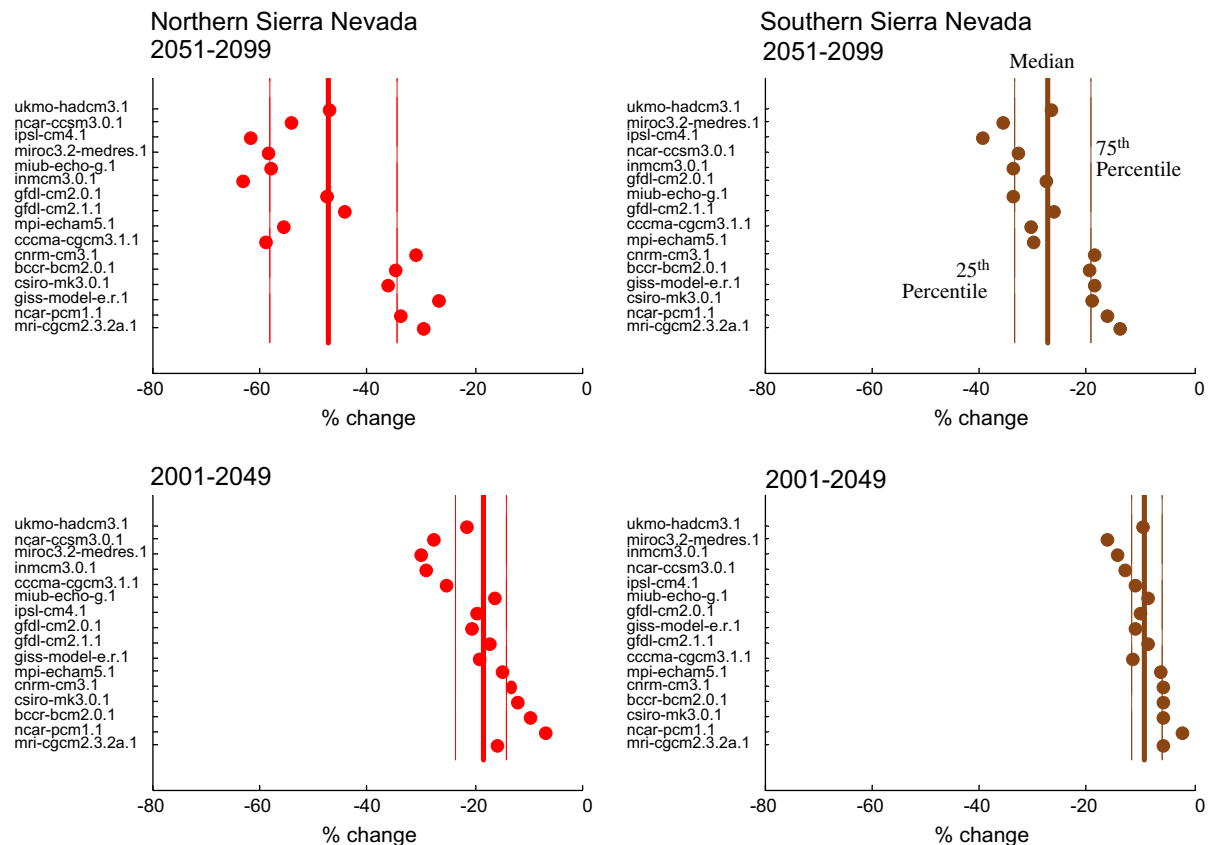
Fig. 8. Changes in annual snow days as a percentage of wet days computed from downscaled global climate model precipitation and temperature. The percentage is calculated from period 1951–1999. The results are averaged over 49-years segments of the 21st century. The heavier solid color vertical line shows the median changes computed from the total model populations. 25th and 75th percentiles values are represented by dotted line. Results are shown from high emission scenario (SRES A2). Climate models in y-axis are sorted based on projected change in mean annual temperature: lowest warming (bottom) and highest warming (top). Left panels: for Northern Sierra Nevada. (For interpretation of the references to colour in this figure legend, the reader is referred to the web version of this article.)

(Das et al., 2009, 2011). The ensemble climate model projections show fewer snowy days in the future, as compared to historical period simulations (Fig. 8).

4. Discussion and conclusions

This study investigated potential changes in magnitude of floods of various return periods in the Sacramento-San Joaquin Valleys that might arise from projected warmer temperatures and changes in precipitation in the 21st Century. Recognizing uncertainties in current climate-change projections, we evaluate floods in an ensemble of climate projections from 16 GCMs forced by two future emission scenarios each. Those projections were statistically downscaled and used to force a macroscale hydrologic model of the Northern and Southern Sierra Nevada. Taken together, the resulting ensemble of hydrologic projections suggests increased projected flood risk in the Northern and Southern Sierra under large majorities of future climate projections, regardless of whether the projected climate is wetter or drier on average. The increases are caused by combinations of changing storm intensities and retreating snowlines.

Our principal findings are:

- The ensemble of climate model projections used here suggests drier conditions for Southern Sierra by end of the 21st century. For Northern Sierra about half of climate model projections show wetter and about half of projection suggest drier conditions. However the changes are small compared to the inter-model variability.

- By the end of the 21st century, all climate model projections yield larger 3-day flood magnitudes for both the Northern and Southern Sierra Nevada, regardless of the direction of change in mean precipitation. In the Northern Sierra, the 50-year flood flows increase (relative to simulated historical values) by 30–90%; in the Southern Sierra, by 50–100%. These changes would be large enough to pose important challenges in terms of infrastructure and flood management. For example, following standard engineering design flood frequency analysis (USGS, 1981), confidence limits are assigned to design floods; for the two composite basins included in this study, the upper 95% confidence interval of the 50-year design flood is 43–59% above the mean. Thus, adapting to the projected increases in 50-year flood flows would be comparable to designing, using historic observations, for the 95% upper confidence limit (or higher) rather than the mean 50-year design flow.

- The ensemble-median 50-year flood magnitude increases progressively through the 21st century, with markedly larger increases in the southern Sierra and under the higher greenhouse gas emission scenario. Under the SRES A2 emissions scenario, by the 49-year period centered on 2025–2035, the increase in the ensemble-median 50-year, 3-day flood peak has increased to exceed the 95% confidence range of historical natural variability.

Changes in flood magnitudes associated with climate changes may pose challenges in California since California's reservoir system is designed to provide not only water storage but also flood protection. Thus, more severe floods would require maintaining

flood reserve volume in key reservoirs, meaning that valuable water might have to be released. This raises the potential for failures of aging levee systems and for disruptions of freshwater conveyances throughout the Central Valley and into southern California. Although uncertainties exist in all steps of this analysis, we have used a large (32 member) ensemble of projections to explore many possible futures to support the conclusion that it is highly likely that flood magnitudes will increase significantly as climate changes in the current century, especially if greenhouse gas emissions remain along a higher trajectory. Notably, the results here are based on GCMs that participated in the CMIP3. With CMIP5 results becoming available, future researchers may wish to compare this analysis with corresponding CMIP5 results. However, there is a strong agreement in temperature projections and general agreement in precipitation projections between the CMIP3 and the CMIP5 in most regions including California, so that differences in flood results may not be large (Knutti and Sedlácek, 2012; Langenbrunner and Neelin, 2013). The present ensemble represents a wide range of futures that nearly all result in increased flood probabilities; CMIP5 futures for the most part are expected to fall within much the same ranges. Even with CMIP5, there will remain many inherent uncertainties shared with earlier assessment results (e.g. Knutti and Sedlácek, 2012). The likelihoods of increasing flood risks appear to be quite real, and planning and investments for flood management in California will benefit from anticipating such changes.

Acknowledgments

References

Anderson, M., Miller, N.L., Heiland, B., King, J., Lek, B., Nemeth, S., Pranger, T., Roos, M., 2006. Climate Change Impacts on Flood Management. Progress on Incorporating Climate change into Management of California's Water Resources. California Department of Water Resources Progress Report. Governor's Climate Initiative Report (Chapter 6).

Barnett, T.P., Pierce, D.W., Hidalgo, H.G., Bonfils, C., Santer, B.D., Das, T., Bala, G., Wood, A.W., Nazawa, T., Mirin, A., Cayan, D.R., Dettinger, M.D., 2008. Human-induced changes in the hydrology of the western United States. Science 319, 1080–1083. http://dx.doi.org/10.1126/science.1152538.

Boé, J., Terray, L., Habets, F., Martin, E., 2007. Statistical and dynamical downscaling of the Seine basin climate for hydro-meteorological studies. Int. J. Climatol. 27, 1643–1655. http://dx.doi.org/10.1002/joc.1602.

Bouwer, L., Vellinga, P., 2003. Changing climate and increasing costs—implications for liability and insurance climatic change: implications for the hydrological cycle and for water management. In: Beniston, M. (Ed.), Advances in Global Change Research. Springer, Netherlands, pp. 429–444.

CA DWR, 2006. Progress on Incorporating Climate Change into Planning and Management of California's Water Resources. Technical Memorandum Report.

CA DWR, 2008. Managing an Uncertain Future; Climate Change Adaptation Strategies for California's Water. California Department of Water Resources, Sacramento, CA.

Carter, T.R., Jones, R.N., Lu, X., Bhadwal, S., Conde, C., Mearns, L.O., O'Neill, B.C., Rounsevell, M.D.A., Zurek, M.B., 2007. New assessment methods and the

characterisation of future conditions. In: Parry, M.L., Canziani, O.F., Palutikof, J.P., van der Linden, P.J., Hanson, C.E. (Eds.), Climate Change 2007: Impacts, Adaptation and Vulnerability. Contribution of Working Group II to the Fourth Assessment Report of the Intergovernmental Panel on Climate Change. Cambridge University Press, Cambridge, UK, pp. 133–171.

Cayan, D.R., Riddle, L., 1992. Atmospheric Circulation and Precipitation in the Sierra Nevada: Proceedings, International Symposium on Managing Water Resources During Global Change. American Water Resources Association, Reno, Nevada, November 1–5.

Cayan, D.R., Dettinger, M.D., Diaz, H.F., Graham, N.E., 1998. Decadal variability of precipitation over Western North America. J. Clim. 11, 3148–3166.

Cayan, D.R., Maurer, E.P., Dettinger, M.D., Tyree, M., Hayhoe, K., 2008a. Climate change scenarios for the California region. Clim. Change 87 (Suppl. 1), 21–42. http://dx.doi.org/10.1007/s10584-007-9377-6.

Cayan, D.R., Lures, A.L., Franco, G., Hanemann, M., Croes, B., Vine, E., 2008b. Overview of the California climate change scenarios project. Clim. Change 87 (Suppl. 1), S1–S6. http://dx.doi.org/10.1007/s10584-007-9352-2.

Cherkauer, K.A., Bowling, L.C., Lettenmaier, D.P., 2003. Variable infiltration capacity cold land process model updates. Global Plan Change 38, 151–159.

Chow, V.T., D. R. Maidment, L.W. Mays, 1988. Applied Hydrology. Mcgraw-Hill International Editions, Civil Engineering Series.

Christensen, J.H., Hewitson, B., Busuioc, A., Chen, A., Gao, X., Held, I., Jones, R., Kolli, R.K., Kwon, W.-T., Laprise, R., Magaña Rueda, V., Mearns, L., Menéndez, C.G., Räisänen, J., Rinke, A., Sarr, A., Whetton, P., 2007. Regional climate projections. In: Solomon, S., Qin, D., Manning, M., Chen, Z., Marquis, M., Averyt, K.B., Tignor, M., Miller, H.L. (Eds.), Climate Change 2007: The Physical Science Basis. Contribution of Working Group I to the Fourth Assessment Report of the Intergovernmental Panel on Climate Change. Cambridge University Press, Cambridge, United Kingdom and New York, NY, USA..

Chung, F., Anderson, J., Arora, S., Ejeta, M., Galef, J., Kadir, T., Kao, K., Olson, A., Quan, C., Reyes, E., Roos, M., Seneviratne, S., Wang, J., Yin, H., Blomquist, N., 2009. Using future climate projections to support water resources decision making in California, California Energy Commission Technical Report CEC-500-2009-052-F, August 2009.

Daly, C., Neilson, R.P., Phillips, D.L., 1994. A statistical-topographic model for mapping climatological precipitation over mountainous terrain. J. Appl. Meteor. 33, 140–158.

Das, T., Hidalgo, H.G., Dettinger, M.D., Cayan, D.R., Pierce, D.W., Bonfils, C., Barnett, T.P., Bala, G., Mirin, A., 2009. Structure and detectability of trends in hydrological measures over the Western US. J. Hydrometeorol. 10, 871–892. http://dx.doi.org/10.1175/2009JHM1095.1.

Das, T., Dettinger, M.D., Cayan, D.R., Hidalgo, H.G., 2011. Potential increase in floods in California's Sierra Nevada under future climate projections. Clim. Change. http://dx.doi.org/10.1007/s10584-011-0298-z.

Dettinger, M.D., 2005. From Climate Change Spaghetti to climate change distributions for 21st Century. San Francisco Estuary Watershed Sci. 3 (1).

Dettinger, M.D., Ingram, B.L., 2013. The coming megafloods. Sci. Am. 308 (1), 64–71.

Dettinger, M.D., Cayan, D.R., Meyer, M.K., Jeton, A.E., 2004. Simulated hydrologic responses to climate variations and change in the Merced, Carson, and American River basins, Sierra Nevada, California, 1900–2099. Clim. Change 62, 283–317.

Dettinger, M., Hidalgo, Hugo, Das, Tapash, Cayan, Daniel, Knowles, Noah., 2009. Projections of Potential Flood Regime Changes in California. Public Interest Energy Research, California Energy Commission, Sacramento, CA.

Easterling, D.R., Karl, T.R., Mason, E.H., Hughes, P.Y., Bowman, D.P., Daniels, R.C., Boden, T.A., 1996. United States Historical Climatology Network (U.S. HCN) Monthly Temperature and Precipitation Data. ORNL/CDIAC-87, NDP-019/R3, Carbon Dioxide Information Analysis Center, 280pp.

Easterling, D.R., Meehl, G.A., Parmesan, C., Changnon, S.A., Karl, T.R., Mearns, L.O., 2000. Climate extremes: observations, modeling, and impacts. Science 2889 (5487), 2068–2074.

Ficklin, D.L., Stewart, I.T., Maurer, E.P., 2012. Projections of 21st Century Sierra Nevada local hydrologic flow components using an ensemble of general circulation models. J. Am. Water Resour. Assoc. 48, 1104–1125, doi: http://dx.doi.org/10.1111/j.1752-1688.2012.00675.

Fowler, H.J., Blenkinsop, S., Tebaldi, C., 2007. Linking climate change modelling to impacts studies: recent advances in downscaling techniques for hydrological modelling. Int. J. Climatol. 27, 1547–1578, 1510.1002/joc.1556.

Friedlingstein, P., Houghton, R.A., Marland, G., Hackler, J., Boden, T.A., Conway, T.J., Canadell, J.G., Raupach, M.R., Ciais, P., Le Quéré, C., 2010. Update on CO_2 emissions (pdf, 147 kb). Nat. Geosci. 3, 811–812.

Girvetz, E.H., Zganjar, C., Raber, G.T., Maurer, E.P., Kareiva, P., Lawler, J.J., 2009. Applied climate-change analysis: the climate wizard tool. PLoS ONE 4, e8320.

Griffis, V.W., Stedinger, J.R., 2007. The log-Pearson type 3 distribution and its application in flood frequency analysis. 1: Distribution characteristics. J. Hydrol. Eng. 12 (5), 482–491.

Groisman, P.Y., Knight, R.W., Easterling, D.R., Karl, T.R., Hegerl, G.C., Razuvaev, V.N., 2005. Trends in intense precipitation in the climate record. J. Clim. 18, 1326–1350.

Haan, C.T., 2002. Statistical Methods in Hydrology, second ed. Iowa State Press, Ames, Iowa, USA, p. 496.

Hamlet, A.F., Lettenmaier, D.P., 2005. Production of temporally consistent gridded precipitation and temperature fields for the continental US. J. Hydromet. 6, 330–336.

Hawkins, E., Sutton, R., 2009. The potential to narrow uncertainty in regional climate predictions. Bull. Am. Met. Soc. 90, 1095–1107.

Hayhoe, K., Cayan, D., Field, C.B., Frumhoff, P.C., Maurer, E.P., Miller, N.L., Moser, S.C., Schneider, S.H., Cahill, K.N., Cleland, E.E., Dale, L., Drapek, R., Hanemann, R.M., Kalkstein, L.S., Lenihan, J., Lunch, C.K., Neilson, R.P., Sheridan, S.C., Verville, J.H., 2007. Emissions pathways, climate change, and impacts on California. Proc. Nat. Acad. Sci. 101, 12422–12427.

Hidalgo, H.G., Das, T., Dettinger, M.D., Cayan, D.R., Pierce, D.W., Barnett, T.P., Bala, G., Mirin, A., Wood, A.W., Bonfils, C., Santer, B.D., Nozawa, T., 2009. Detection and attribution of climate change in streamflow timing of the Western United States. J. Clim. 22 (13), 3838–3855.

Jain, S., Lall, U., Mann, M.E., 1999. Seasonality and interannual variations of Northern Hemisphere temperature: equator-to-pole gradient and ocean–land contrast. J. Clim. 12, 1086–1100.

Kalnay, E., and Coauthors, 1996: The NCEP/NCAR 40-Year Reanalysis Project. Bull. Amer. Meteor. Soc., 77, 437–471.

Kelley, R., 1998. Battling the inland sea—floods, public policy and the Sacramento Valley. University of California Press, 420p.

Knowles, N., Dettinger, M., Cayan, D., 2006. Trends in snowfall versus rainfall for the Western United States. J. Clim. 19, 4545–4559.

Knutti, R., Sedlácek, J., 2012. Robustness and uncertainties in the new CMIP5 climate model projections. Nat. Clim. Change. http://dx.doi.org/10.1038/nclimate1716.

Kunkel, K.E., Karl, T.R., Easterling, D.R., Redmond, K., Young, J., Yin, X., Hennon, P., 2013. Probable maximum precipitation (PMP) and climate change. Geophys. Res. Lett. 40. http://dx.doi.org/10.1002/grl.50334.

Langenbrunner, B., David Neelin, J., 2013. Analyzing ENSO Teleconnections in CMIP Models as a Measure of Model Fidelity in Simulating Precipitation. J. Climate 26, 4431–4446. http://dx.doi.org/10.1175/JCLI-D-12-00542.1.

Liang, X., Lettenmaier, D.P., Wood, E.P., Burges, S.J., 1994. A simple hydrologically based model of land surface water and energy fluxes for GSMs. J. Geophys. Res 99 (D7), 14415–14428.

Lohmann, D., Nolte-Holube, R., Raschke, E., 1996. A large scale horizontal routing model to be coupled to land surface parameterization schemes. Tellus 48A, 708–721.

Lund, J.R., 2012. Flood management in California. Water 4, 157–169. http://dx.doi.org/10.3390/w4010157.

Mailhot, A., Duchesne, S., 2010. Design criteria of urban drainage infrastructures under climate change. J. Water Resour. Plan. Manage 136, 201, doi: 10.1061/(ASCE)WR.1943-5452.0000023.

Maurer, E.P., 2007. Uncertainty in hydrologic impacts of climate change in the Sierra Nevada, California under two emissions scenarios. Clim. Change 82 (3–4), 309–325. http://dx.doi.org/10.1007/s10584-006-9180-9.

Maurer, E.P., Wood, A.W., Adam, J.C., Lettenmaier, D.P., Nijssen, B., 2002. A long-term hydrologically-based data set of land surface fluxes and states for the conterminous United States. J. Clim. 15, 3237–3251.

Maurer, E.P., Brekke, L., Pruitt, T., Duffy, P.B., 2007. Fine-resolution climate change projections enhance regional climate change impact studies. Eos Trans. Am. Geophys. Union 88, 504, doi: 510.1029/2007EO470006.

Maurer, E.P., Hidalgo, H.G., Das, T., Dettinger, M.D., Cayan, D.R., 2010. The utility of daily large-scale climate data in the assessment of climate change impacts on daily streamflow in California. Hydrol. Earth Syst. Sci. 14, 1125–1138. http://dx.doi.org/10.5194/hess-14-1125-2010.

Miller, N.L., Bashford, K.E., Strem, E., 2003. Potential impacts of climate change on California hydrology. J. Am. Water Resour. Assoc., 771–784.

Milly, P.C.D., Wetherald, R.T., Dunne, K.A., Delworth, T.L., 2002. Increasing risk of great floods in a changing climate. Nature 415, 514–517.

Min, S.-K., Zhang, X., Zweirs, F.W., Hegerl, G.C., 2011. Human contribution to more intense precipitation extremes. Nature 470, 378–381. http://dx.doi.org/10.1038/nature09763.

Morandi, L., 1998. Water Table—Negotiating the Bay-Delta Accord. National Conference of State Legislatures, Denver, 16p.

Neiman, P.J., Ralph, F.M., Wick, G.A., Lundquist, J.D., Dettinger, M.D., 2007. Meteorological characteristics and overland precipitation impacts of atmospheric rivers affecting the west coast of North America Based on Eight Years of SSM/I. J. Hydrometeorol. 9, 22–47.

Panofsky, H.A., Brier, G.W., 1968. Some Applications of Statistics to Meteorology. The Pennsylvania State University, University Park, PA, USA, 224pp.

Pielke Jr., R.A., Downton, M.W., Barnard Miller, J.Z., 2002. Flood Damage in the United States, 1926–2000: A Reanalysis of National Weather Service Estimates. UCAR, Boulder, CO.

Pierce, D.W., Das, T., Cayan, D.R., Maurer, E.P., Miller, N., Bao, Y., Kanamitsu, M., Yoshimura, K., Snyder, M.A., Sloan, L.C., Franco, G., Tyree, M., 2013a. Probabilistic estimates of future changes in California temperature and precipitation using statistical and dynamical downscaling. Clim. Dynam. 40 (3–4), 839–856. http://dx.doi.org/10.1007/s00382-012-1337.

Pierce, D.W., Cayan, D.R., Das, T., Maurer, E.P., Miller, N.L., Bao, Y., Kanamitsu, M., Yoshimura, K., Snyder, M.A., Sloan, L.C., Franco, G., Tyree, M., 2013b. The key role of heavy precipitation events in climate model disagreements of future annual precipitation changes in California. J. Clim.. http://dx.doi.org/10.1175/jcli-d-12-00766.1.

Raff, D.A., Pruitt, T., Brekke, L.D., 2009. A framework for assessing flood frequency based on climate projection information. Hydrol. Earth Syst. Sci. 13 (1–18).

Ralph, F.M., Neiman, P.J., Wick, G.A., Gutman, S.I., Dettinger, M.D., Cayan, D.R., White, A.B., 2006. Flooding on California's Russian River: role of atmospheric rivers. Geophys. Res. Lett. 33, L13801. http://dx.doi.org/10.1029/2006GL026689.

Reis Jr., D.S., Stedinger, J.R., Martins, E.S., 2005. Bayesian generalized least squares regression with application to log Pearson type 3 regional skew estimation. Water Resour. Res. 41, W10419. http://dx.doi.org/10.1029/2004WR003445.

Service, R.F., 2007. Environmental restoration—Delta blues, California style. Science 317, 442–445.

Themeßl, M.J., Gobiet, A., Heinrich, G., 2012. Empirical-statistical downscaling and error correction of regional climate models and its impact on the climate change signal. Clim. Change 112, 449–468. http://dx.doi.org/10.1007/s10584-011-0224-4.

Trenberth, K.E., 1999. Conceptual framework for changes of extremes of the hydrological cycle with climate change. Clim. Change 42, 327–339.

US Department of Agriculture, 2011. California Agricultural Statistics, <http://www.nass.usda.gov/Statistics_by_State/California/Publications/California_Ag_Statistics/Reports/2009cas-all.pdf> (accessed 17.08.11).

USGS, 1981. Guidelines for Determining Flood flow Frequency, U.S. Department of Interior, U.S. Geological Survey, Interagency Committee on Water Data, Bulletin 17B of the Hydrology Subcommittee, Reston Virginia.

Wood, A.W., Maurer, E.P., Kumar, A., Lettenmaier, D.P., 2002. Long-range experimental hydrologic forecasting for the eastern United States. J. Geophys. Res. Atmos. 107. http://dx.doi.org/10.1029/2001jd000659.

Wood, A.W., Leung, L.R., Sridhar, V., Lettenmaier, D.P., 2004. Hydrologic implications of dynamical and statistical approaches to downscaling climate model outputs. Clim. Change 62, 189–216.